Scientia Horticulturae 321 (2023) 112337

Contents lists available at ScienceDirect

Scientia Horticulturae

journal homepage: www.elsevier.com/locate/scihorti

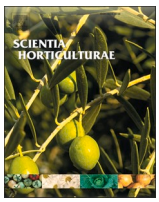

Genetic and geographical inputs that shape Metabolomic and transcriptomic profiles of melon fruits

Seyednami Niyakan [a,b,1], Yukihiro Nagashima [b,c,1], Jashbir Singh [b,c], Rita Metrani [b,c], Kevin M. Crosby [b,c], John L. Jifon [b,c,d], GK Jayaprakasha [b,c], Sadhana Ravishankar [b,e], Paul Brierley [b,f], Daniel I. Leskovar [b,g], Thomas A. Turini [b,h], Jonathan Schultheis [b,i], Timothy Coolong [b,j], Wenjing Guan [b,k], Rhonda Miller [b,l], Bhimanagouda Patil [b,c,m], Xiaoning Qian [a,b,n,o], Hisashi Koiwa [b,c,p,*]

[a] Department of Electrical and Computer Engineering, Texas A&M University, College Station, TX 77843, USA
[b] United States Department of Agriculture National Center of Excellence, USA
[c] Vegetable and Fruit Improvement Center, Department of Horticultural Sciences, Texas A&M University, College Station, TX 77843, USA
[d] Texas A&M AgriLife Research and Extension Center, 2415 E Business 83, Weslaco, TX 78596, USA
[e] School of Animal and Comparative Biomedical Sciences, University of Arizona, 1117 E. Lowell Street, Tucson, AZ 85721, USA
[f] Yuma Center of Excellence for Desert Agriculture, University of Arizona, Yuma, Arizona 85364, USA
[g] Texas A&M AgriLife Research and Extension Center, Department of Horticultural Sciences, Texas A&M System, 1619 Garner Field Road, Uvalde, TX 78801, USA
[h] University of California Cooperative Extension, Fresno, CA 93710, USA
[i] Department of Horticultural Sciences, North Carolina State University, Raleigh, NC 27695, USA
[j] Department of Horticulture, University of Georgia, Athens, GA 30602, USA
[k] Department of Horticultural and Landscape Architecture, Purdue University, 625, Agriculture Mall Drive, West Lafayette, IN 47907, USA
[l] Department of Animal Science, Texas A&M University, College Station, TX 77843, USA
[m] Department of Food Science and Technology, Texas A&M University, College Station, TX 77843, USA
[n] TEES-AgriLife Center for Bioinformatics & Genomic Systems Engineering, Texas A&M University, College Station, TX 77843, USA
[o] Department of Computer Science and Engineering, Texas A&M University, College Station, TX 77843, USA
[p] Molecular and Environmental Plant Sciences, Texas A&M University, College Station, TX 77843, USA

ARTICLE INFO

Keywords:
Cucumis melo
Fruit
Aromatic volatiles
Metabolites
Transcriptome
Association analysis
Sensory analysis
Flavors
QTL

ABSTRACT

Melon (*Cucumis melo*) is an important crop grown worldwide. The diversity of aromatic volatiles melon fruits produce contributes to their diverse flavors. However, little is known about the chemical and molecular profiles essential for establishing the signature flavors in field conditions. Here we analyzed the metabolome and transcriptome of 10 melon varieties grown in the field in Weslaco, TX. Also, two cultivars (TTDV and F39) grown at seven locations in the US were studied further to understand how geographic conditions influence levels of metabolites and transcripts. The data obtained here were combined with sensory data, and the relationship between observed metabolites/transcripts and fruit quality QTL was evaluated. Overall, esters and lipid-derived metabolites varied significantly in different sample sets. TTDV variety was significantly enriched for esters, whereas honeydew varieties were for lipid-derived metabolites, separating their profiles from other varieties. Among transcripts associated with cultivar-specific metabolites, we identified several transcripts linked to QTLs responsible for the production of fruit metabolites, including *benzyl alcohol O-benzoyltransferase* (*AAT2*) and *caffeic acid 3-O-methyltransferase 1-like*. On the other hand, transcripts associated with location-specific metabolites did not produce a clear overlap with known fruit-quality QTLs, suggesting the presence of different regulatory systems for the environmental control of fruit metabolites.

* Corresponding author at: Vegetable and Fruit Improvement Center, Department of Horticultural Sciences, Texas A&M University, College Station, TX 77843, USA.
E-mail address: hisashi.koiwa@ag.tamu.edu (H. Koiwa).
[1] These authors contributed equally.

https://doi.org/10.1016/j.scienta.2023.112337
Received 24 April 2023; Received in revised form 10 July 2023; Accepted 12 July 2023
Available online 26 July 2023

1. Introduction

Melons (*Cucumis melo*), including cantaloupe and honeydew, are important horticultural crops of the Cucurbitaceae family, with global annual production reaching around 27 million tons. Fruits of melons produce a wide variety of metabolites that generate the unique aroma of fruits. Aromatic profiles of melon fruits change not only over the development and maturation of fruits but also by varieties and growth conditions. Because fruit aroma is a crucial component of determining fruit quality and consumer preferences, the growth management and harvest practices that affect fruit aroma can influence the success of crop production. Regulation of volatile organic compounds (VOC) production in fruits is an integral component of the development of fruit aroma and varies substantially between climacteric and non-climacteric varieties. Climacteric ripening produces a peak of ethylene biosynthesis accompanied by increased respiration, which is lacking in non-climacteric varieties (Lelièvre et al., 1997). Climacteric melon fruits are rich in aroma, and non-climacteric melons produce less fruit aroma (Allwood et al., 2014; Gonda et al., 2016). Metabolomic studies confirmed that different melon varieties are associated with unique aromatic signatures (Allwood et al., 2014; Bernillon et al., 2013; Moing et al., 2020; Wu et al., 2022), which reflects phylogenomic relationships of the varieties (Moing et al., 2020). A melon homolog of tomato *NON-RIPENING* (*NOR*) is essential for the climacteric ripening of melon fruit. A CRISPR-induced melon *nor-1* mutant did not produce ethylene and was prevented from climacteric ripening (Liu et al., 2022). VOC production was significantly reduced in the *nor-1* mutant, indicating that VOC production is indeed regulated as a part of the integrated climacteric ripening process (Liu et al., 2022).

Melon VOCs mainly consist of aldehydes, alcohols, esters, terpenoids, apocarotenoids, thioesters, lactones, and phenolics. These compounds are derived from lipids, amino acids, phenolics, terpenoids, and carotenoids (Gonda et al., 2016). The *nor-1* fruits produced significantly less esters and more lipid-derived aldehydes and terpenes, consistent with the increase of esters during the maturation of fruits (Liu et al., 2022). Through spatiotemporal metabolomics, Mori et al. (2019) showed that metabolic adjustment based on O_2 demand and O_2 availability is essential for the proper maturation of the fruit . Consistently, fermentation and ethanol production induced by hypoxia in fruit mesocarp are integral to ethyl ester production (Biais et al., 2010). In addition to the aromatic quality, some metabolites can also affect the visual appearance of the fruits. Carotenoid levels directly affect the fresh color of fruits (Chayut et al., 2021; Diao et al., 2023; Esteras et al., 2018; Freilich et al., 2015), whereas flavonoids could affect fruit skin colors (Zhang et al., 2021). (Diao et al., 2023) Metabolomic and transcriptomic analyses have been increasingly used to monitor dynamic changes in fruit metabolites and underlining gene expressions during the ripening of melon fruits. Metabolomic studies typically focus on within-fruit position specificity (Biais et al., 2009, 2010), ripening time course (Moing et al., 2011a), fruit varieties (Allwood et al., 2014; Lee et al., 2014; Moing et al., 2020), and grafting effects (Zhang et al., 2019) whereas transcriptome studies ripening time course (Nagashima et al., 2021; Schemberger et al., 2020; Shin et al., 2017; Zhang et al., 2016), varieties (Freilich et al., 2015; Girelli et al., 2018; Saladié et al., 2015), postharvest treatments (Ning et al., 2022), and grafting effects (Chen et al., 2021). Surprisingly, only a handful of studies addressed the relationship between chemical and molecular components regulating various aromatic profiles of melon fruits (Freilich et al., 2015; Galpaz et al., 2018; Lee et al., 2014; Nagashima et al., 2021). Also, the impact of production geography on melon fruit's metabolome or transcriptome has not been addressed extensively (Bernillon et al., 2013).

Melon is diploid (2n = 24) and has an approximate genome size of 450 Mbp (Arumuganathan and Earle, 1991). A high-quality reference genome of melon (DHL92 v4.0) covers 358 Mbp pseudomolecules (Castanera et al., 2020; Garcia-Mas et al., 2012). Several mapping and association analyses have been performed to detect quantitative trait locus (QTL) regulating important fruit traits at the gene resolution, but few studies have investigated the association of fruit metabolites to QTLs regulating the traits at the gene resolution (Freilich et al., 2015; Galpaz et al., 2018; Oren et al., 2022). In this study, metabolome, transcriptome datasets, and sensory datasets were prepared from melon fruits of ten different cultivars grown in Weslaco, TX. Datasets were also produced from two cultivars grown in the field at seven US locations. Cultivar- and location-associated metabolites were identified and used to determine gene sets that mimic the expression profile of the metabolites. The biological significance of selected genes was confirmed because they included genes corresponding to QTLs influencing the levels of fruit-quality-related metabolites. These results laid a foundation to integrate various analytical platforms to understand the complex network of fruit quality traits in melons.

2. Materials and methods

2.1. Materials

Melon fruits analyzed in this study included muskmelon cultivars, namely: a Western-shipper type F39 (Chujuc; TAMU), Tuscan type (Da Vinci, TTDV; Sakata Seed America, USA), Harper-type Infinite Gold (HT-IG, Sakata Seed America, Inc), Primo (PRI, Stokes, USA), Cruiser (CRU, Moran Seed Co, USA), and hybrids (TH5 and TH6, TAMU) and honeydew varieties HD150 (TAMU), HD252 (Nunhems Seed Co., USA) and Orange Cassava (OC, TAMU). The plants were grown during the spring growing season (March–June 2019) in fields located at the Texas A&M AgriLife Research Center – Texas A&M University System in Weslaco, Texas (latitude 26° 9′ N, longitude 97° 57′ W; elevation 21 m) as described previously (Nagashima et al., 2021). In addition, F39 and TTDV plants were grown in TX (Uvaldi, harvest years 2018 and 2019), GA, NC, CA, IN, and AZ in 2019. Due to the harvesting schedules, we could not include F39 samples from the Indiana location in our analysis. The growth condition of each location was reported previously (Singh et al., 2022). Fruits were harvested at maturity (approximately 45 days after flowering).

2.2. Metabolite analysis

Fruit metabolite datasets analyzed were a part of metabolome datasets collected in Texas A&M University for USDA specialty crop research initiative, which were obtained as described previously (Metrani et al., 2022, 2023; Singh et al., 2020, 2021, 2022). After the quantification of GC–MS data, metabolite concentration levels were pre-processed to impute the true expression values into the zero values in the dataset. Mean-imputation was applied to zero values in the GC–MS dataset, as reported previously (Nagashima et al., 2021, 2022; Singh et al., 2020). Principal Component Analysis (PCA) (Wold et al., 1987) was performed on the imputed metabolite expression datasets by the factoextra package in R (v1.0.7) (Kassambara and Mundt, 2020).

Differential Expression (DE) analysis was done on the imputed metabolite data to detect cultivar- and location-specific metabolites. To perform DE analysis, we used the Voom function implemented in the Limma package (v3.52.3) (Ritchie et al., 2015). For cultivar samples, metabolite expression levels across the ten varieties were compared pairwise to identify significant differences in metabolite expression values. Subsequently, for each metabolite for each cultivar, scores (0 to 9) were assigned based on the number of significant pairwise DE results. The same procedure was applied for location-specific samples, and metabolites were scored 0 to 6 for pairwise comparisons of seven locations.

2.3. Sensory analysis

Odor, flavor, and texture descriptive attribute evaluations were conducted with seven expert-trained sensory panelists (IRB number:

IRB-2017–0524). Sensory flavor aromatic (melon identity, overall sweet, musty earth, honey, green, overripe, fermented), basic tastes (sweet, sour, bitter), and texture (surface moisture, hardness, and juiciness) attributes were evaluated using 16-point scales (0=none, no surface moisture, soft, and dry; 15=extremely intense, extremely wet surface, extremely hard, and extremely juicy) as defined in Table 1. Panelists were trained for two weeks on identifying attributes, and references were presented during training and testing. Panelists were provided with saltless saltine crackers and double-distilled, deionized water as pallet cleansers between samples (Bett-Garber et al., 2005; Vallone et al., 2013). During training, panelists were served commercially purchased melons, and the consensus was obtained for each attribute across samples served.

During testing, melons were cut to remove the rind and seed cavity. From three melons, 1.25 cm cores were removed from the melon's flesh to represent the fruit. Cores were mixed from the three melons, and five randomly selected cores were placed in glass custard cups with glass concave lids labeled with random three-digit codes for each panelist. Within a sensory day, samples were randomized to order, and samples were served at least four minutes apart to reduce sensory fatigue. Panelists were seated in individual booths under white light (44.2 lux) separated from the sample preparation area, and up to 12 samples were presented per day. Panelists evaluated texture attributes using two fruit cores, and flavor aromatics and basic tastes were evaluated on the remaining three.

2.4. RNA-seq analysis

Total RNA extraction and RNA-seq library preparation were performed using Universal RNA-Seq Library Preparation Kit with NuQuant (Tecan, Switzerland) as described previously (Nagashima et al., 2021, 2022). NGS sequencing run was performed using the NovaSeq platform for 150 nucleotides paired-end analysis. Reads were aligned to the Melonomics genome sequence: CM3.6.1_pseudomol.fa (https://www.melonomics.net/melonomics.html#/download) along with the annotation reference: CM4.0.gtf, using STAR (v2.5.4b) (Dobin et al., 2013) with two allowed mismatches per pair at maximum for the alignment (outFilterMismatchNmax=2), which successfully generated 6.3–34.2 million aligned reads per fruit corresponding to 61–91% of the total sequence reads per fruit. Raw and aligned NGS data were deposited to GEO (Accession number GSE228039). Weslaco F39 and TTDV datasets (samples S59-S64, from GSE178084) used in the previous report (Nagashima et al., 2021, 2022) were analyzed together in this study. The uniquely mapped reads were used to count the number of reads per gene while mapping, considering overlapping one and only one gene according to its genome location. Both ends of the paired-end reads were checked for overlaps.

The raw RNA-seq expression data were then pre-processed by filtering out the transcripts with count per million (CPM) below 1 (low expressed transcripts). Then, the data were normalized following the DESeq function implemented in the DESeq2 R package (v1.36.0) (Love et al., 2014) after adjusting for the known biological melon sample covariates of cultivar location, fruit type, and binary TRSV (Tabara et al., 2021) contamination status. The binary TRSV contamination status of samples was determined by checking for any unmapped TRSV sequences in melon fruit sample sequences. Following the instructions from DESeq2 in Love et al. (2014), we then performed variance stabilizing transformation (VST) (Tibshirani, 1988) on the RNA-seq data by the vst function implemented in the DESeq2 package.

Table 1
Sensory attributes of cantaloupes.

Attribute	Definition
Flavor Aromatics	
Melon Identity	The aromatics associated with melons
Overall Sweet	The combination of sweet taste and sweet aromatics
Honey	Sweet, light brown, slightly spicy aromatic associated with honey
Green	Sharp, slightly pungent aromatics associated with green/ plant/vegetable matters such as parsley, spinach, pea pod, fresh cut grass, etc.
Musty/Earthy	The somewhat sweet, heavy aromatic associated with decaying vegetation and damp, black soil
Overripe fruit, near fermented	The sweet, slightly sour, damp, musty/earthy aromatic characteristic of fruit or vegetable past their optimum ripeness
Fermented	The pungent, sweet, slightly sour, sometimes yeasty, alcohol-like aromatic characteristic of fermented fruits or sugar or over-proofed dough
Basic Tastes	
Sweet	The fundamental taste factor associated with sucrose
Bitter	The fundamental taste factor associated with a caffeine solution
Sour	The fundamental taste factor associated with citric acid
Texture	
Surface Moisture	The amount of moisture on the surface
Hardness	The force to compress between molars,
Juiciness	The amount of juice/ moisture perceived in the mouth

2.5. Association analysis

In order to identify transcripts co-regulated with sample-specific metabolites, we designed an association analysis pipeline. We followed the normalization and transformation process explained in the previous section while keeping all the low-expressed genes. For the association analysis, we kept the top 10,000 genes with the highest variance of their expression values across fruit samples and filtered out the rest. For each cultivar- or location-specific metabolite set that we identified by our metabolite analysis pipeline, we searched for any significant co-regulation between the transcripts and each of the metabolites in the corresponding metabolite set based on statistical significance analysis of the fitted ridge regression model with each metabolite expression as the dependent variable and transcriptomic expression values as independent variables. We performed this analysis using the linearRidge function implemented in the ridge R package (v3.3) (Cule and De Iorio, 2013). After the model fitting, we considered the transcripts with the corresponding regression coefficient p-values lower than the significance threshold 0.01 as significantly co-regulated with the considered metabolite. Transcripts are considered co-regulated with a set of either cultivar- or location-specific metabolites if they were identified as correlated with more than half the number of metabolites in the set.

Gene set enrichment analysis (GSEA) for metabolite-associated transcripts was performed by the hypeR package (v2.0.1) (Federico and Monti, 2020), and the melon pathways were extracted from Cucurbit Genomics Database (CuGenDB) (Zheng et al., 2019).

3. Results

3.1. Overview and clustering of cultivar datasets

Metabolic profiling and sensory data were used to establish relationships between the fruit's chemical and sensory properties (Supplementary Data 1, Table 1). The data were visualized by principal component analysis (PCA) (Fig. 1). Overall, the plot showed clustering of honeydew varieties (HD150, HD252, and OC164), hybrids (TH5 and TH6), and loose clustering of cantaloupes (CRU, PRIM, F39, and HTIG). However, TTDV was substantially distant from all the varieties. Honeydew varieties were positively associated with sensory parameters "Green" and "Sour." Hybrids were associated with "Juiciness," "Surface moisture," and "Fermented." And cantaloupes except TTDV were associated with "MelonID," "Honey," "Overall sweetness," and "Overripe." TTDV was negatively associated with "Juiciness," "Surface moisture," and "Fermented."

Cultivar-specific metabolites were identified by differential expression analysis. Levels of each metabolite in different cultivars were scored

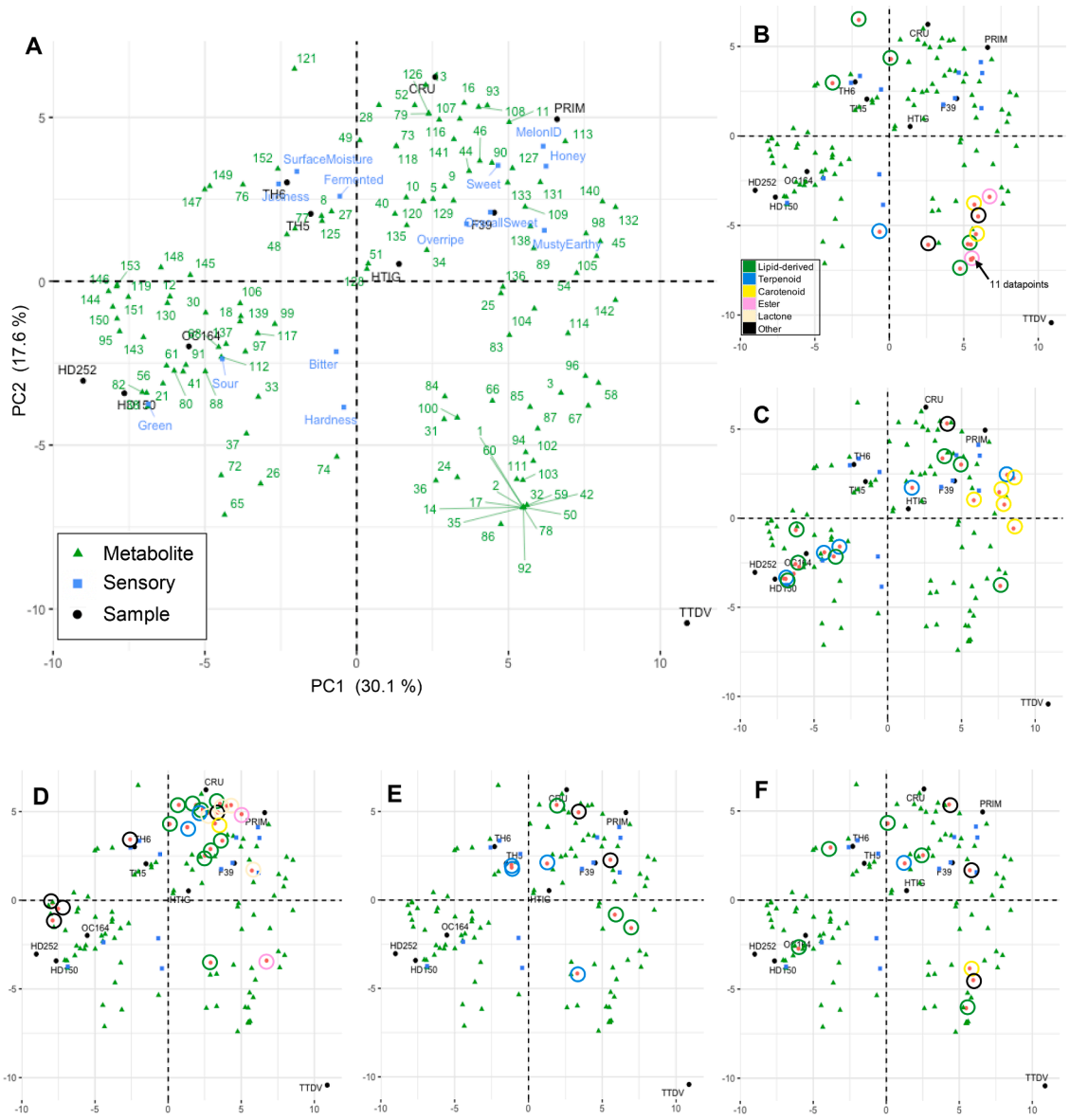

Fig. 1. Principal component analysis of metabolites and sensory traits in different melon cultivars grown in Weslaco, TX in 2019. A) Master Biplot showing score plot and loading plot. Cultivar-specific metabolites were highlighted in B) TTDV set C) honeydew set (HD150, HD252, OC164), D) Primo/Cruser set E)TH set F) F39 set. Explained variance for PC1 and PC2 are indicated as the percentages in the X- and Y-axis, respectively.

using a 0–9 scale, where 0 indicated no significant difference against other varieties, and 9 indicated significant differences against all nine other varieties (Supplemental Data 2). Highly ranked metabolites were extracted and highlighted in Fig. 1B-Fig. 1F and the levels of metabolites were visualized by heatmap analysis (Fig. 2). Based on the relative abundance, these metabolites were classified as significantly enriched or significantly depleted (SEM and SDM). The TTDV profile was characterized by ester SEM and lipid-derived SDM (Fig. 1B, 2A). Honeydew varieties (HD150, HD252, OC164) were associated with lipid-derived and mono and sesquiterpenoid SEM and carotenoid SDM (Fig. 1C, 2B). Primo and Cruiser (PRI and CRU) showed similar overall profiles and were enriched with lipid-derived volatiles and sesquiterpenoids (Fig. 1D, 2C). Hybrid varieties (TH5, TH6) do not have clear trends but have two monoterpene SEMs (limonene and eudesmol) (Fig. 1E, 2D). SEM and SDM for F39 often overlap with other cultivars, and only a small number of metabolites, mainly lipid-derived SDM volatiles, were detected as significant (Fig. 1F, 2E). Infinite Gold (HTIG) metabolite profile was plotted close to the origin in the PCA and did not produce metabolites with high significance (Fig. 1A).

3.2. Location-specific metabolites in TTDV and F39

Location-specific fruit metabolites were identified using two cultivars. TTDV was selected for its unique profile, whereas F39 was chosen because it frequently shared metabolites of significance with other varieties. The metabolite and sensory data collected from fruits grown in 7 US locations in 2018 (Uvalde, TX) and 2019 (all locations: Uvalde, TX; Weslaco, TX, Arizona, California, Georgia, Indiana, North Carolina) were processed, and SEM and SDM were identified (Supplemental Data 3). The resulting PCA data were plotted (Fig. 3A), and SEM and SDM for each location were mapped on the PCA plot (Fig. 3B-3F). The levels of location-specific SEM/SDM were visualized in heap maps (Fig. 4). The Georgia samples showed ester SEMs and carotenoid SDMs (Fig. 4A). Uvalde, TX samples showed ester SEMs and amino acid SDMs (Fig. 4B). Weslaco, TX samples lipid derivative SEM and terpenoid SDM (Fig. 4C). Only a few metabolites were identified for Indiana, Arizona, and California samples (Fig. 4D-G). North Carolina samples showed variety-specific behaviors but were generally associated with lipid-derived SDM and terpenoid metabolites (both SEM and SDM) (Fig. 4D).

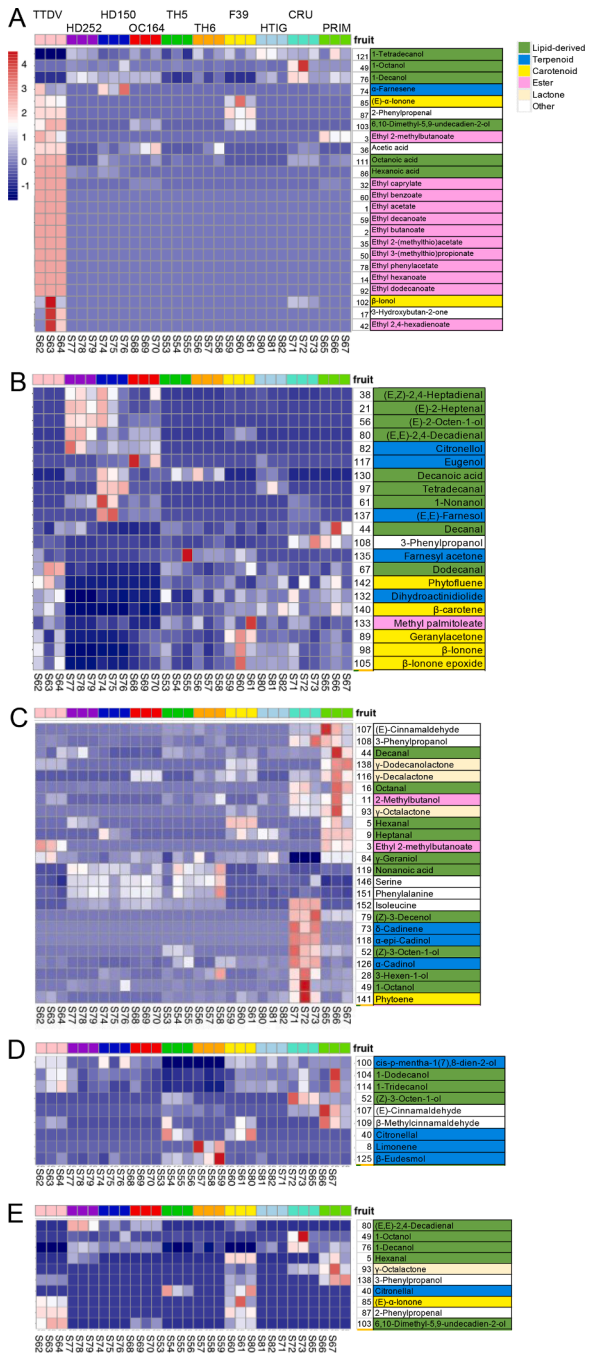

Fig. 2. Heatmap showing levels of cultivar-specific metabolites in different melon fruits in TTDV (A), Honeydew (B) Primo/Cruiser (C) TH (D) and F39 (E). The normalized Z-score values of metabolite levels (μg/kg fresh weight) were used to generate the heatmap.

3.3. Analysis of cultivar and location-specific gene expression

The above metabolite analyses indicated that each cultivar and geographic location of production promote a unique set of metabolites in the fruit aroma. We next determined transcripts uniquely associated with each cultivar- or location-specific blend of metabolites using RNA-seq dataset for each fruit analyzed above. The RNA was prepared separately from triplicate samples used in the metabolite analysis. The sequencing run produced a total of 450 Gbases of paired-end data, corresponding to 1.5 billion reads for 68 samples. After filtering the reads for contaminating TRSV sequences (Nagashima et al., 2021; Tabara et al., 2021), sequence reads were aligned to the melon reference genome (CM.4.0pseudomol.fa) using STAR (v2.5.2b) (Dobin et al., 2013). This successfully generated 6.3–34.2 million aligned reads per fruit corresponding to 61–91% of the total sequence reads per fruit (Supplemental Data 4). A normalized transcriptome dataset for each fruit was used for the PCA plot together with the previous dataset for the fruit maturation time course (Nagashima et al., 2021, 2022). As seen in Fig. 5, the new fruit set (purple) clustered together with late-stage samples (green) in the PCA plot, indicating that the sample set used in this study was well-matured at the harvest time.

To obtain insights into gene expression patterns relevant to the formation of phytochemicals, we investigated the expression of a set of genes in phytochemical biosynthesis pathways (Supplementary Figs. 1 and 2). The key metabolites included lipids, terpenoids, carotenoids, phenolics/esters, and fermentation. Two types of heatmaps for gene expression were produced, one based on the expression level (cpm value) and the other scaled relative to other samples (Z score). The expression profile was inspected to identify connections with characteristic metabolic profiles of TTDV and honeydews described above. The gene expression patterns in metabolic pathways were similar across the cultivars. However, some significant differential expressions were detected. In TTDV, higher expression levels were observed in *MELO3C004253* (*9-lipoxygenase 7*) and *MELO3C018833* (*13-hydroperoxide lyase*), and *MELO3C018413* (*9/13-hydroperoxide lyase*) in lipid metabolism pathway, *MELO3C029738* (*Terpene cyclase/mutase family member*) in terpenoid pathway, *MELO3C025102, MELO3C016185,* and *MELO3C014677* (*Phytoene synthase*), *MELO3C020832* (*15-cis-phytoene desaturase*), *MELO3C017709* (*zeta-carotene isomerase*) and *MELO3C023555* (*Carotenoid cleavage dioxygenase (CCD) 1*) in the carotenoid pathway, *MELO3C024766* (*alcohol acyltransferase*), *MELO3C018492* (*cinnamyl alcohol dehydrogenase 4/5*) in phenolics/esters pathway. In honeydew varieties, higher expression levels were observed in *MELO3C024348* (*13-lipoxygenase 18*) and *MELO3C023687, MELO3C002189*, and *MELO3C026553* (*alcohol dehydrogenase*), and *MELO3C024414* and *MELO3C012886* (*3Z:2E-Enal Isomerases*) in lipid metabolism pathway, *MELO3C020952* (*Geranylgeranyl diphosphate synthase)*, MELO3C017709 (*zeta-carotene isomerase*), *MELO3C024674* (*zeta-carotene desaturase*) in terpenoid/carotenoid pathway, *MELO3C024769* (*alcohol acyltransferase*), *MELO3C017061, MELO3C009963*, and *MELO3C010188* (*cinnamoyl-CoA reductase*), *MELO3C019548* (*cinnamyl alcohol dehydrogenase*), *MELO3C016208* (*coniferyl alcohol acetyltransferase*), and *MELO3C023304* (*eugenol synthase*) in phenolics/esters pathway, and *MELO3C019503* (*alcohol dehydrogenase*) in fermentation pathway.

Heatmap analysis of representative metabolic pathway gene expressions for F39 and TTDV grown at different locations produced relatively uniform profiles. Unexpectedly, overall transcript levels, including lipoxygenases and other oxylipin-related genes in samples from Weslaco with several lipid-derived SEM, were not significantly different from samples from other locations. However, some increases were detected in *9/13-hydroperoxide lyase* (*MELO3C018413*), which could be responsible for the increase in (Z,Z)−3,6-nonadienal concentration, and in *4-coumarate-CoA ligase* in Weslaco F39 samples (Supplementary Fig. 2, Fig. 4C). Georgia F39 samples showed a moderate increase in *phenylalanine ammonia lyases (PAL), hydroxycinnamoyl-CoA: shikimate/quinate hydroxycinnamoyltransferase,* and *p-coumaroyl shikimate/quinate 3′-hydroxylase,* which are components of phenylpropanoid pathway leading to monolignol productions. Uvalde samples produced profiles with elevated *LOX, PAL,* and *4-coumarate-CoA ligase* isoforms (Supplementary Fig. 2).

Since structural genes in metabolite pathways showed limited sample-specific trends, to empirically identify transcripts co-regulated with sample-specific metabolites, we performed an association analysis of transcripts using the accumulation patterns of sample-specific metabolites as queries. For F39, TTDV, HD, TH, and PC metabolite datasets, we identified 60, 886, 83, 9, and 46 genes co-regulated with the sample-specific metabolites suites. Similarly, for the location

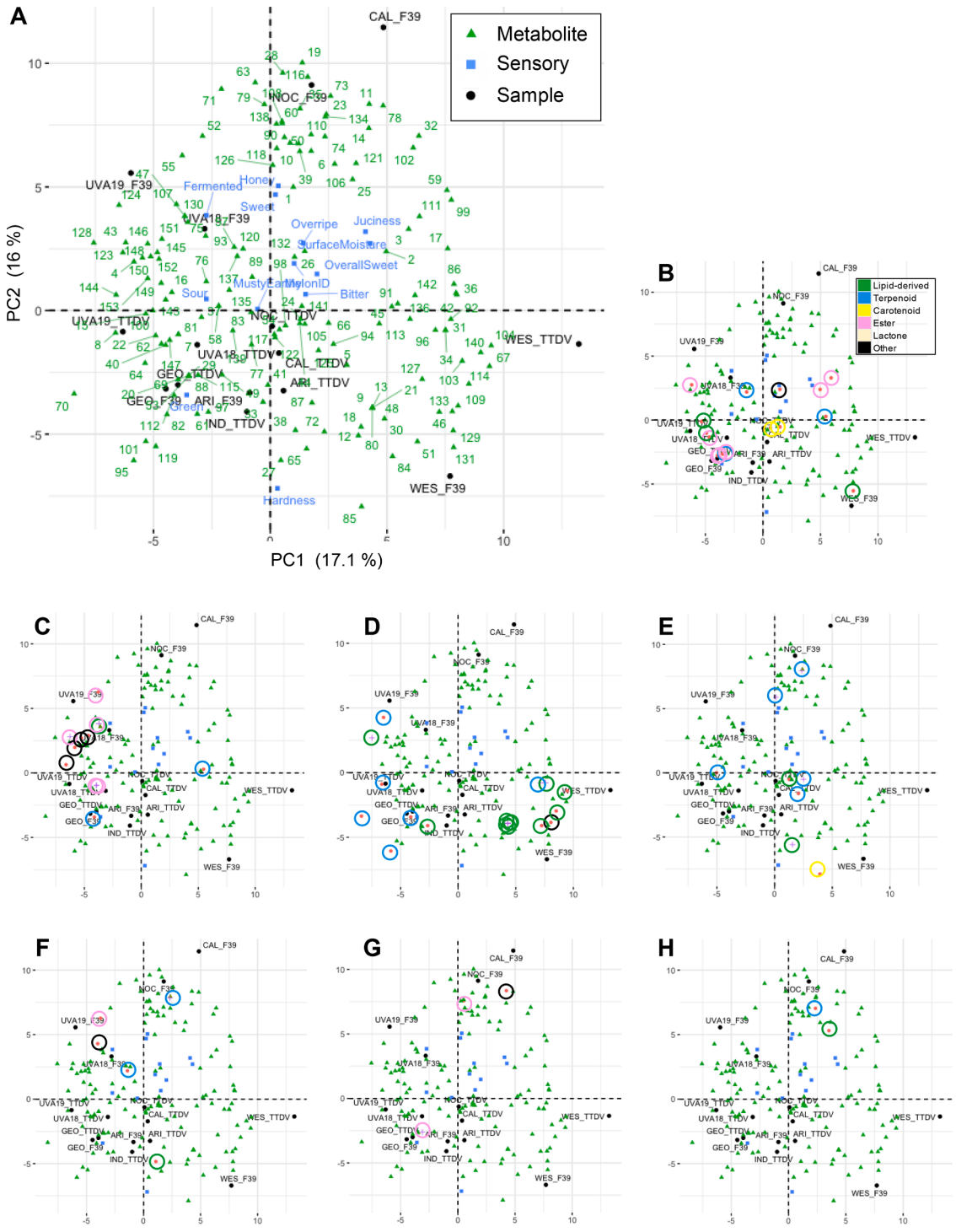

Fig. 3. Principal component analysis of metabolites and sensory traits in melon fruit (TTDV and F39) grown in different US locations in 2018 and 2019. A) Master Biplot showing score plot and loading plot. Location-specific metabolites (orange dots) were highlighted in B) Georgia set C) Uvaldi, TX set, D) Weslaco, TX set E) North Carolina set F) California se. G) Indiana set, and H) Arizona set. Explained variance for PC1 and PC2 are indicated as the percentages in the X- and Y-axis, respectively. "+" indicates variety specific accumulation in the location.

dataset, 7, 50, 80, 61, 52, 31, 15, and 41 genes were identified for Georgia, Uvaldi 2019, Uvaldi 2018, Weslaco, North Carolina, California, Arizona, and Indiana sample sets, respectively (Supplemental Data 5, 6). The metabolite-associated transcripts were subjected to gene set enrichment analysis (GSEA) to identify upregulated pathways in a specific cultivar or growth location. GSEA-identified gene sets for metabolic pathways were also limited and represented by only one gene for most cases. However, amino acid metabolism pathways were observed multiple times, most prevalently in the TTDV data set, in which 19 gene sets related to amino acid metabolism were identified with $P<0.1$ for two or more genes (Supplemental Table 1). From the location-dataset analysis, the UVA18 sample (S47-S52) was enriched for glycolysis and lipid biosynthesis pathways. Genes in o-diquinones biosynthesis found in Uvalde samples in both 2018 and 2019 datasets are likely polyphenol oxidases, suggesting activation of wounding/oxidative stress response in the fruits.

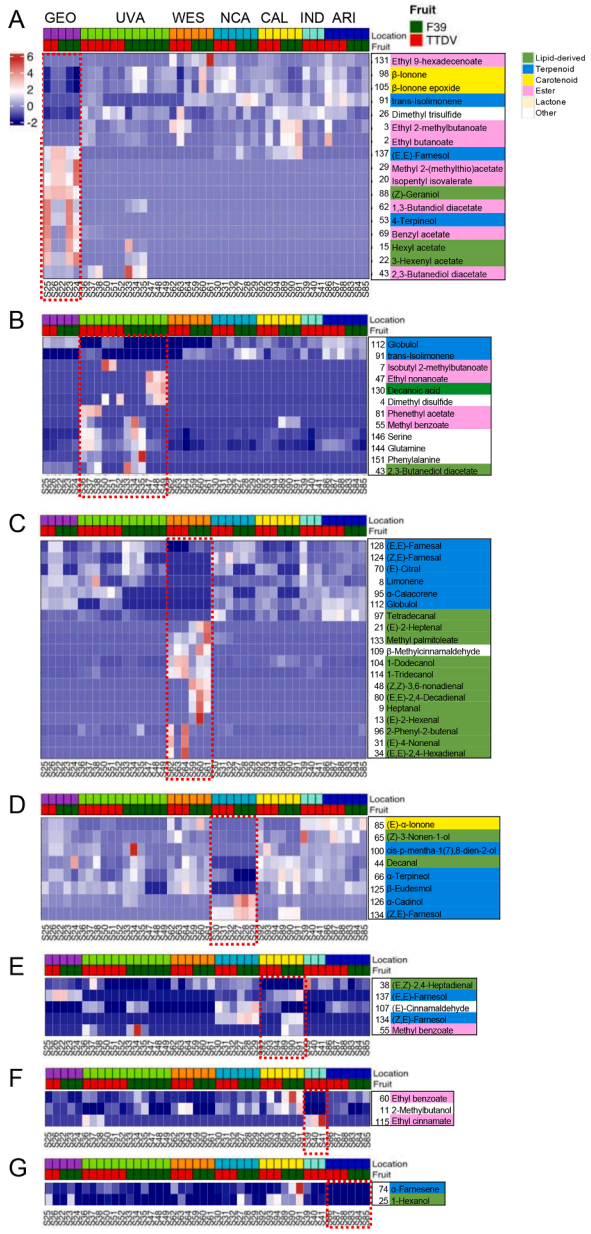

Fig. 4. Heatmap showing levels of location-specific metabolites in melon fruits harvested in different US locations. Metabolites specific for A) Georgia (GEO), B) Uvaldi (UVA), TX, C)Weslaco (WES), TX, D)North Carolina (NOC), E) California (CAL), F) Indiana (IND), and G) Arizona (ARI) are shown. Red boxes indicate specific location for the metabolite sets. Numbers next to metabolites indicate ID numbers in PCA plots (Figs. 1 and 3). The normalized Z-score values of metabolite levels (μg/kg fresh weight) were used to generate the heatmap.

3.4. Relationship between metabolite-associated genes and QTLs

Metabolite-associated gene set for each sample was used as a query to determine if they represented fruit-quality QTL (Fig. 6). We used previously reported fruit-quality QTL data (Freilich et al., 2015; Galpaz et al., 2018) for data mining of metabolite-associated transcripts for linked QTL (Table 2). Genes in a QTL peak containing two or fewer genes were used for analysis. With the HD variety-associated transcripts, only *MELO3C014088* (*caffeic acid 3-O-methyltransferase 1-like*) was associated with QTL peak for total carotenoid levels (r^2=0.169, (Galpaz et al., 2018)). TTDV dataset included several transcripts mapped to fruit-quality-related QTLs. Most notably, *MELO3C024766* (*benzyl alcohol O-benzoyltransferase, alcohol acyltransferases; AAT2*) has been associated with QTL for volatile esters: ethyl 3-(methylthio)propanoate, ethyl tiglate and ethyl 2-methylbutanoate with r^2= 0.242, 0.18, and 0.183, respectively (Galpaz et al., 2018). Additionally, *MELO3C004423* (*protease 2*) was associated with benzoic acid, *MELO3C009790* (*15-cis-phytoene desaturase*) with methyl benzoate, *MELO3C016581* (*C2H2-like zinc finger protein*) with α-cadinene, *MELO3C014578* (*Protein RETICULATA-RELATED 4*) with sucrose, *MELO3C020296* (*2-isopropylmalate synthase 2*) with S-methyl thiobutanoate, and *MELO3C014089* (*caffeic acid 3-O-methyltransferase 1-like*) with total carotenoids, and *MELO3C015422* (*arginine-tRNA ligase*) with α-carotene, respectively. Furthermore, *MELO3C019694* (*AGAMOUS MADS-box factor transcription factor)* associated with sutures (Zhao et al., 2019) was also identified in TTDV. In F39, *MELO3C013865* (*ubiquitin family protein*) for 1-phenethyl alcohol and β-carotene was identified. By contrast, the location-associated dataset contained only three fruit-associated QTL: *MELO3C009615* (*RING/U-box superfamily protein*) for methyl cinnamate and *MELO3C006875* (*BCL-2-associated athanogene 3*) for sucrose and β-elemene in North Carolina dataset, and *MELO3C025265* (*auxin efflux career*) for 3-phenylpropyl acetate and fructose in Primo/Cruser dataset.

The lack of identified QTL associated with location-specific datasets may indicate a rather subtle environmental influence or indirect regulation of the expression of the phenotype through QTL. We, therefore, searched for regulators (eQTL) that may target metabolite-associated QTL (Galpaz et al., 2018). Using this analysis, two transcripts were identified in UVA-dataset: *MELO3C011891* (*lysine histidine transporter*) targeting *MELO3C011876* for total carotenoid and *MELO3C008033* (*RING-H2 finger protein ATL78*) for 3-phenylpropyl acetate (Galpaz et al., 2018).

4. Discussion

Diverse metabolic pathways are responsible for producing aromas associated with fruit qualities. As a part of United States Department of Agriculture-Specialty Crop Research Initiative project, we have conducted multi-cultivar and multi-location growth trials of cantaloupe and honeydew melons, which were followed by multifaceted analyses including metabolitome, transcriptome, and sensory analyses. Changes in specific metabolite groups have been observed in the trial, and were reported previously (Metrani et al., 2022, 2023; Singh et al., 2020, 2021, 2022). In this study, we used a metabolite and transcript profiling approach to analyze a suite of melon fruit samples, including ten varieties, of which two were grown in seven different US locations. The maturity stage of each fruit was confirmed by PCA analysis of transcriptome data plotted together with the maturity time-course transcriptome data reported previously. Metabolome data highlighted variety-specific profiles, which were also associated with sensory test results. By contrast, the diversity of metabolite profiles among the same varieties grown at different locations was relatively small. Several cases showed more significant separations among varieties and years grown in the same location than the samples of the same variety grown in different locations.

Differential expression analysis of variety and location-specific fruit metabolites showed a clear trend of enrichment of metabolites in the same major categories, such as esters, lipid derivatives, and terpenoids, as clusters. Furthermore, opposite trend was found for esters and lipid derivatives in TTDV samples (Fig. 2A). A similar reciprocal trend was observed when a metabolite profile of *nor-1* (*no ripening*) was compared with the wild-type metabolite profile (Liu et al., 2022). Enrichment of ethyl esters in TTDV may indicate high fermentation activity and an anaerobic environment in the fruits, as indicated by a spatial metabolomics study (Moing et al., 2011b). Various linear and branched organic acids were used to form fruit esters. These are derived from primary metabolites, including pyruvic acid, amino acids, and lipids. Nevertheless, the molecular mechanism of forming many of these metabolites is poorly understood. Pyruvate decarboxylase 1 (PDC1) is

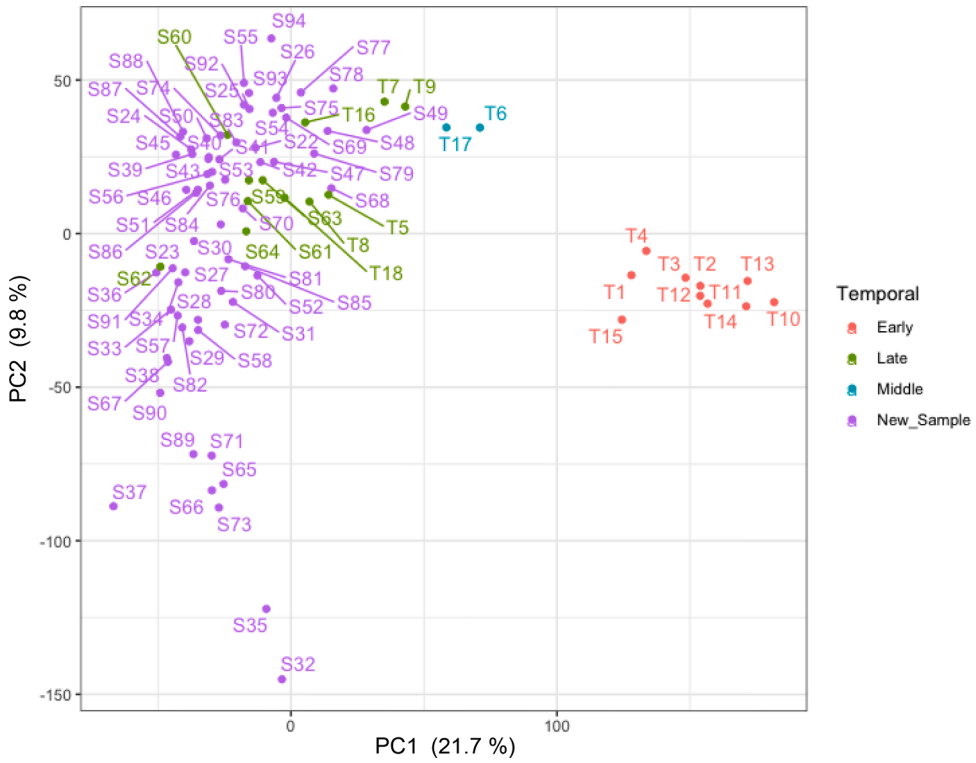

Fig. 5. Global assessment of transcriptomic data from melon fruit samples. PCA analysis was conducted for the new datasets together with time course dataset (TTDV and F39) analyzed previously (Nagashima et al., 2021). New datasets cluster with late-stage datasets.

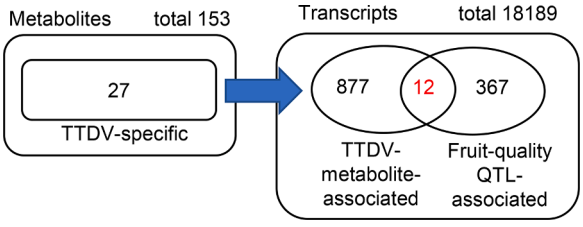

Fig. 6. Summary of association analysis for TTDV-specific data. Expression pattern of TTDV specific metabolites across the samples were used to identify TTDV specific transcripts coregulated with the query metabolites. Metabolite-associated transcripts for TTDV were used to search fruit-quality QTL-associated genes to identify QTL-encoded transcripts coregulated with TTDV metabolites.

responsible for the production of some linear esters but not for branched-chain esters (Wang et al., 2019). Differentially expressed esters identified in this study include ones likely derived from branched-chain amino acid biosynthesis pathway, such as leucine (isopentyl isovalerate) and isoleucine (Ethyl 2-methylbutanoate), and from methionine (Ethyl 3-(methylthio)propionate), but specific enzymes/genes responsible for the biosynthesis have yet to be identified.

Various lipid-derived volatile aldehydes and alcohols are produced via the combined function of lipoxygenases (LOX) and hydroperoxy lyases (HPL). They are enriched in honeydew varieties and also in Weslaco locations, promoting "Green" unripe flavors. Z,Z-3,6-Nonadienal, associated with cucumber odor, was enriched in Weslaco samples. These often-undesirable metabolites can be suppressed to improve fruit aroma by silencing LOX and HPL. Our data suggested several candidates for specific LOX and HPL isoforms, such as *MELO3C004253* (*9-LOX*) *MELO3C010910/MELO3C008413* (*9/13-HPL*), for further investigations.

Extraction of cultivar-specific, metabolite-associated transcripts in TTDV data identified ten genes strongly linked with previously detected fruit-quality QTLs, which can affect total carotenoid content, volatile aromatic esters, and terpenoids. These QTLs have been previously proposed to control 11–44% differences in the population (Galpaz et al., 2018). Interestingly, in the detected QTL, we observed genes in phenylpropanoid or esters/phenolics production encoding a QTL for carotenoid levels and vice versa. The interaction of carotenoid and phenolics biosynthesis pathway/signaling has been reported in maize during seed development (Hattori et al., 1992) and involves ABA signaling. Also, it is notable that tandemly located *MELO3C014088* and *MELO3C014089* encoding *caffeic acid 3-O-methyltransferase 1-like proteins* linked to a carotenoid QTL were detected in datasets for honeydew, a low-carotenoid variety, and TTDV, a high carotenoid variety. In addition, transcripts for QTL responsible for sucrose levels and suture were detected. Furthermore, TTDV-specific transcripts showed enrichment of amino acid biosynthesis pathways. Together, the metabolic and transcript profiles support a flavor-rich quality of the TTDV variety. The consistent fruit quality of TTDV grown in different locations relative to that of F39 was also observed in the clustered profiles on the PCA plot for location-specific datasets. Consistent with the small variability, no transcripts linked to fruit quality QTL peaks were detected from the location dataset, and only weak eQTLs, which may indirectly regulate fruit quality, were detected for carotenoid and esters in UVA-specific transcripts.

In summary, our analysis revealed a more significant contribution of cultivar-specific inputs than growth-location inputs into metabolic profiles affecting fruit qualities. We were able to identify several metabolite-associated transcripts corresponding to QTL contributing to the levels of the relevant metabolites, indicating the potential for combining metabolome and transcriptome data for identifying genetic factors controlling fruit flavors. On the other hand, gene sets identified in our analysis contained many genes after filtering, and currently, *ab initio* identification of flavor determinants without guidance from previously identified QTL information was proven to be difficult. Currently, our dataset is somewhat limited in cultivar numbers and growth trials, therefore, future expansion of datasets could improve our analysis

Table 2
Metabolite-associated transcripts linked to QTL.

sample set	Gene in QTL peak[a]	Annotation	Metabolite for QTLa	r^2 [a]
HD	MELO3C014088	caffeic acid 3-O-methyltransferase 1-like	total carotenoids	0.169
TTDV	MELO3C025265	unknown	fructose	0.255
			3-phenylpropyl acetate	0.268
	MELO3C024766	benzyl alcohol O-benzoyltransferase	3-(methylthio) propanol	0.175
			ethyl 3-(methylthio)propanoate	0.242
			ethyl tiglate	0.18
			ethyl 2-methylbutanoate	0.183
	MELO3C020296	2-isopropylmalate synthase 2, chloroplastic-like	S-methyl thiobutanoate	0.174
	MELO3C015422	Arginine–tRNA ligase	α-carotene	0.154
	MELO3C014089	caffeic acid 3-O-methyltransferase 1-like	total carotenoids	0.169
	MELO3C014578	Protein RETICULATA-RELATED 4, chloroplastic	sucrose	0.166
	MELO3C017332	Stress up-regulated Nod 19	Weight	0.179
	MELO3C016581	C2H2-like zinc finger protein	α-cadinene	0.438
	MELO3C004423	protease 2	benzoic acid	0.137
	MELO3C012960	BZIP protein, putative	benzyl acetate	0.11
	MELO3C009790	15-cis-phytoene desaturase, chloroplastic/chromoplastic	methyl benzoate	0.12
	MELO3C019694[b]	AGAMOUS MADS box factor transcription factor	sutures	N/A
F39	MELO3C013865	ubiquitin family protein	1-phenethyl alcohol	0.079
			β-carotene	0.094
Primo/Cruiser	MELO3C025265	Auxin efflux career	3-phenylpropyl acetate	0.268
			fructose	0.255
North Carolina	MELO3C009615	RING/U-box superfamily protein	methyl cinnamate	0.132
	MELO3C006875	BCL-2-associated athanogene 3	sucrose, β-elemene	0.082

[a] Galpaz et al. (2018). [b]Zhao et al. (2019).

power for a broader range of traits.

4.1. Contribution

Seyednami Niyakan: Investigation, Data curation and analysis, Manuscript writing, Yukihiro Nagashima: Investigation, Data curation and analysis, Manuscript writing, Jashbir Singh: Investigation, Data curation and analysis, Manuscript writing, Rita Metrani: Investigation, Data curation and analysis, Kevin M. Crosby: Resources, John Jifon: Resources, GK Jayaprakasha: Investigation, Data curation and analysis, Sadhana Ravishankar: Resources, Paul Brierley: Resources, Daniel I. Leskovar: Resources, Thomas A. Turini: Resources, Jonathan Schultheis: Resources, Timothy Coolong: Resources, Wenjing Guan: Resources, Rhonda Miller Investigation, Data curation and analysis, Bhimanagouda Patil Investigation, Supervision, Project administration, Xiaoning Qian Investigation, Data curation and analysis, Manuscript writing, Hisashi Koiwa Investigation, Data curation and analysis, Manuscript writing

Funding

This research was funded by the United States Department of Agriculture-NIFA-SCRI- 2017–51181–26834 through the National Center of Excellence for Melon at the Vegetable and Fruit Improvement Center of Texas A&M University. X Qian was supported in part by National Science Foundation awards CCF-1553281, IIS-1812641, and IIS-2212419.

Supplementary materials

Supplementary Table 1: Gene set enrichment analysis of metabolite-associated transcripts

Supplementary Figure 1: Heatmap analysis of biosynthetic pathway gene expression in various melon cultivars

Supplementary Figure 2: Heatmap analysis of biosynthetic pathway gene expression in TTDV and F39 fruits grown in 7 US locations.

Supplementary Data 1: Metabolites and sensory data

Supplementary Data 2: Ranking of cultivar-specific metabolites

Supplementary Data 3: Ranking of Location-specific metabolites

Supplementary Data 4: Summary of RNA-seq data and alignment statistics

Supplementary Data 5: Metabolite-associated transcripts (cultivar)

Supplementary Data 6: Metabolite-associated transcripts (location)

Declaration of Competing Interest

The authors declare the following financial interests/personal relationships which may be considered as potential competing interests:

Bhimanagouda Patil reports financial support was provided by US Department of Agriculture. Xiaoning Qian reports financial support was provided by National Science Foundation

Data availability

Data will be made available on request.

Acknowledgment

We would like to thank Drs. Charlie Johnson and Richard Metz (Texas AgriLife Research Genomics and Bioinformatics Service) for their assistance with RNA-Seq data analysis.

Supplementary materials

Supplementary material associated with this article can be found, in the online version, at doi:10.1016/j.scienta.2023.112337.

References

Allwood, J.W., Cheung, W., Xu, Y., Mumm, R., De Vos, R.C., Deborde, C., Biais, B., Maucourt, M., Berger, Y., Schaffer, A.A., Rolin, D., Moing, A., Hall, R.D., Goodacre, R., 2014. Metabolomics in melon: a new opportunity for aroma analysis. Phytochemistry 99, 61–72. https://doi.org/10.1016/j.phytochem.2013.12.010.

Arumuganathan, K., Earle, E.D., 1991. Nuclear DNA content of some important plant species. Plant Mol. Biol. Rep. 9, 208–218. https://doi.org/10.1007/BF02672069.

Bernillon, S., Biais, B., Deborde, C., Maucourt, M., Cabasson, C., Gibon, Y., Hansen, T.H., Husted, S., de Vos, R.C.H., Mumm, R., Jonker, H., Ward, J.L., Miller, S.J., Baker, J. M., Burger, J., Tadmor, Y.a., Beale, M.H., Schjoerring, J.K., Schaffer, A.A., Rolin, D., Hall, R.D., Moing, A., 2013. Metabolomic and elemental profiling of melon fruit quality as affected by genotype and environment. Metabolomics 9, 57–77. https://doi.org/10.1007/s11306-012-0429-1.

Bett-Garber, K.L., Lamikanra, O., Lester, G.E., Ingram, D.A., Watson, M.A., 2005. Influence of soil type and storage conditions on sensory qualities of fresh-cut cantaloupe (Cucumis melo). J. Sci. Food Agric. 85, 825–830. https://doi.org/10.1002/jsfa.1970.

Biais, B., Allwood, J.W., Deborde, C., Xu, Y., Maucourt, M., Beauvoit, B., Dunn, W.B., Jacob, D., Goodacre, R., Rolin, D., Moing, A., 2009. 1H NMR, GC-EI-TOFMS, and

data set correlation for fruit metabolomics: application to spatial metabolite analysis in melon. Anal. Chem. 81, 2884–2894. https://doi.org/10.1021/ac9001996.
Biais, B., Beauvoit, B., William Allwood, J., Deborde, C., Maucourt, M., Goodacre, R., Rolin, D., Moing, A., 2010. Metabolic acclimation to hypoxia revealed by metabolite gradients in melon fruit. J. Plant Physiol. 167, 242–245. https://doi.org/10.1016/j.jplph.2009.08.010.
Castanera, R., Ruggieri, V., Pujol, M., Garcia-Mas, J., Casacuberta, J.M., 2020. An improved melon reference genome with single-molecule sequencing uncovers a recent burst of transposable elements with potential impact on. Genes. Front. Plant Sci. 10 https://doi.org/10.3389/fpls.2019.01815, 1815-1815.
Chayut, N., Yuan, H., Saar, Y., Zheng, Y., Sun, T., Zhou, X., Hermanns, A., Oren, E., Faigenboim, A., Hui, M., Fei, Z., Mazourek, M., Burger, J., Tadmor, Y., Li, L., 2021. Comparative transcriptome analyses shed light on carotenoid production and plastid development in melon fruit. Hortic Res 8, 112. https://doi.org/10.1038/s41438-021-00547-6.
Chen, S., Li, Y., Zhao, Y., Li, G., Zhang, W., Wu, Y., Huang, L., 2021. iTRAQ and RNA-Seq analyses revealed the effects of grafting on fruit development and ripening of oriental melon (Cucumis melo L. var. makuwa). Gene 766, 145142. https://doi.org/10.1016/j.gene.2020.145142.
Cule, E., De Iorio, M., 2013. Ridge regression in prediction problems: automatic choice of the ridge parameter. Genet. Epidemiol. 37, 704–714. https://doi.org/10.1002/gepi.21750.
Diao, Q., Tian, S., Cao, Y., Yao, D., Fan, H., Zhang, Y., 2023. Transcriptome analysis reveals association of carotenoid metabolism pathway with fruit color in melon. Sci. Rep. 13, 5004. https://doi.org/10.1038/s41598-023-31432-y.
Dobin, A., Davis, C.A., Schlesinger, F., Drenkow, J., Zaleski, C., Jha, S., Batut, P., Chaisson, M., Gingeras, T.R., 2013. STAR: ultrafast universal RNA-seq aligner. Bioinformatics 29, 15–21. https://doi.org/10.1093/bioinformatics/bts635.
Esteras, C., Rambla, J.L., Sanchez, G., Lopez-Gresa, M.P., Gonzalez-Mas, M.C., Fernandez-Trujillo, J.P., Belles, J.M., Granell, A., Pico, M.B., 2018. Fruit flesh volatile and carotenoid profile analysis within the Cucumis melo L. species reveals unexploited variability for future genetic breeding. J. Sci. Food Agric. 98, 3915–3925. https://doi.org/10.1002/jsfa.8909.
Federico, A., Monti, S., 2020. hypeR: an R package for geneset enrichment workflows. Bioinformatics 36, 1307–1308. https://doi.org/10.1093/bioinformatics/btz700.
Freilich, S., Lev, S., Gonda, I., Reuveni, E., Portnoy, V., Oren, E., Lohse, M., Galpaz, N., Bar, E., Tzuri, G., Wissotsky, G., Meir, A., Burger, J., Tadmor, Y., Schaffer, A., Fei, Z., Giovannoni, J., Lewinsohn, E., Katzir, N., 2015. Systems approach for exploring the intricate associations between sweetness, color and aroma in melon fruits. BMC Plant Biol. 15 https://doi.org/10.1186/s12870-015-0449-x, 71-71.
Galpaz, N., Gonda, I., Shem-Tov, D., Barad, O., Tzuri, G., Lev, S., Fei, Z., Xu, Y., Mao, L., Jiao, C., Harel-Beja, R., Doron-Faigenboim, A., Tzfadia, O., Bar, E., Meir, A., Sa'ar, U., Fait, A., Halperin, E., Kenigswald, M., Fallik, E., Lombardi, N., Kol, G., Ronen, G., Burger, Y., Gur, A., Tadmor, Y., Portnoy, V., Schaffer, A.A., Lewinsohn, E., Giovannoni, J.J., Katzir, N., 2018. Deciphering genetic factors that determine melon fruit-quality traits using RNA-Seq-based high-resolution QTL and eQTL mapping. Plant J. 94, 169–191. https://doi.org/10.1111/tpj.13838.
Garcia-Mas, J., Benjak, A., Sanseverino, W., Bourgeois, M., Mir, G., González, V.M., Hénaff, E., Câmara, F., Cozzuto, L., Lowy, E., Alioto, T., Capella-Gutiérrez, S., Blanca, J., Cañizares, J., Ziarsolo, P., Gonzalez-Ibeas, D., Rodríguez-Moreno, L., Droege, M., Du, L., Alvarez-Tejado, M., Lorente-Galdos, B., Melé, M., Yang, L., Weng, Y., Navarro, A., Marques-Bonet, T., Aranda, M.A., Nuez, F., Picó, B., Gabaldón, T., Roma, G., Guigó, R., Casacuberta, J.M., Arús, P., Puigdomènech, P., 2012. The genome of melon (Cucumis melo L.). Proc. Natl. Acad. Sci. U. S. A. 109, 11872–11877. https://doi.org/10.1073/pnas.1205415109.
Girelli, C.R., Accogli, R., Del Coco, L., Angilè, F., De Bellis, L., Fanizzi, F.P., 2018. 1H-NMR-based metabolomic profiles of different sweet melon (Cucumis melo L.) Salento varieties: analysis and comparison. Food Res. Int. 114, 81–89. https://doi.org/10.1016/j.foodres.2018.07.045.
Gonda, I., Burger, Y., Schaffer, A.A., Ibdah, M., Tadmor, Y.a., Katzir, N., Fait, A., Lewinsohn, E., 2016. Biosynthesis and perception of melon aroma. Biotechnol. Flavor Prod. 281–305. https://doi.org/10.1002/9781118354056.ch11.
Hattori, T., Vasil, V., Rosenkrans, L., Hannah, L.C., McCarty, D.R., Vasil, I.K., 1992. The Viviparous-1 gene and abscisic acid activate the C1 regulatory gene for anthocyanin biosynthesis during seed maturation in maize. Genes Dev. 6, 609–618. https://doi.org/10.1101/gad.6.4.609.
Kassambara, A., Mundt, F., 2020. Factoextra: extract and visualize the results of multivariate data analyses. R Package Version 1.0.7. https://CRAN.R-project.org/package=factoextra.
Lee, J., Kim, M.K., Hwang, S.H., Kim, J., Ahn, J.M., Min, S.R., Park, S.U., Lim, S.S., Kim, H., 2014. Phenotypic profiling and gene expression analyses for aromatic and volatile compounds in Chamoes (Cucumis melo). Mol. Biol. Rep. 41, 3487–3497. https://doi.org/10.1007/s11033-014-3211-9.
Lelièvre, J.M., Latchè, A., Jones, B., Bouzayen, M., Pech, J.C., 1997. Ethylene and fruit ripening. Physiol. Plant 101, 727–739.
Liu, B., Santo Domingo, M., Mayobre, C., Martín-Hernández, A.M., Pujol, M., Garcia-Mas, J., 2022. Knock-Out of CmNAC-NOR affects melon climacteric fruit ripening. Front. Plant Sci. 13 https://doi.org/10.3389/fpls.2022.878037.
Love, M.I., Huber, W., Anders, S., 2014. Moderated estimation of fold change and dispersion for RNA-seq data with DESeq2. Genome Biol. 15 https://doi.org/10.1186/s13059-014-0550-8, 550-550.
Metrani, R., Jayaprakasha, G.K., Patil, B.S., 2022. Optimization of experimental parameters and chemometrics approach to identify potential volatile markers in seven cucumis melo varieties using HS–SPME–GC–MS. Food Anal. Methods 15, 607–624. https://doi.org/10.1007/s12161-021-02119-9.
Metrani, R., Singh, J., Jayaprakasha, G.K., Crosby, K.M., Jifon, J.L., Ravishankar, S., Brierley, P.E., Leskovar, D.I., Turini, T.A., Schultheis, J., Coolong, T., Guan, W., Patil, B.S., 2023. Multi-location evaluation of cantaloupe (Cucumis melo L.) cultivars for their aroma and flavor related volatile composition using a metabolomics approach. Food Chem. Adv. 2, 100223 https://doi.org/10.1016/j.focha.2023.100223.
Moing, A., Aharoni, A., Biais, B., Rogachev, I., Meir, S., Brodsky, L., Allwood, J.W., Erban, A., Dunn, W.B., Kay, L., de Koning, S., de Vos, R.C., Jonker, H., Mumm, R., Deborde, C., Maucourt, M., Bernillon, S., Gibon, Y., Hansen, T.H., Husted, S., Goodacre, R., Kopka, J., Schjoerring, J.K., Rolin, D., Hall, R.D., 2011a. Extensive metabolic cross-talk in melon fruit revealed by spatial and developmental combinatorial metabolomics. New Phytol. 190, 683–696. https://doi.org/10.1111/j.1469-8137.2010.03626.x.
Moing, A., Aharoni, A., Biais, B., Rogachev, I., Meir, S., Brodsky, L., Allwood, J.W., Erban, A., Dunn, W.B., Kay, L., de Koning, S., de Vos, R.C.H., Jonker, H., Mumm, R., Deborde, C., Maucourt, M., Bernillon, S., Gibon, Y., Hansen, T.H., Husted, S., Goodacre, R., Kopka, J., Schjoerring, J.K., Rolin, D., Hall, R.D., 2011b. Extensive metabolic cross-talk in melon fruit revealed by spatial and developmental combinatorial metabolomics. New Phytol. 190, 683–696. https://doi.org/10.1111/j.1469-8137.2010.03626.x.
Moing, A., Allwood, J.W., Aharoni, A., Baker, J., Beale, M.H., Ben-Dor, S., Biais, B., Brigante, F., Burger, Y., Deborde, C., Erban, A., Faigenboim, A., Gur, A., Goodacre, R., Hansen, T.H., Jacob, D., Katzir, N., Kopka, J., Lewinsohn, E., Maucourt, M., Meir, S., Miller, S., Mumm, R., Oren, E., Paris, H.S., Rogachev, I., Rolin, D., Saar, U., Schjoerring, J.K., Tadmor, Y., Tzuri, G., de Vos, R.C.H., Ward, J. L., Yeselson, E., Hall, R.D., Schaffer, A.A., 2020. Comparative metabolomics and molecular phylogenetics of melon (Cucumis Melo, Cucurbitaceae) biodiversity. Metabolites 10. https://doi.org/10.3390/metabo10030121.
Mori, K., Beauvoit, B.P., Biais, B., Chabane, M., Allwood, J.W., Deborde, C., Maucourt, M., Goodacre, R., Cabasson, C., Moing, A., Rolin, D., Gibon, Y., 2019. Central metabolism is tuned to the availability of oxygen in developing melon fruit. Front. Plant Sci. 10, 594. https://doi.org/10.3389/fpls.2019.00594.
Nagashima, Y., He, K., Singh, J., Metrani, R., Crosby, K.M., Jifon, J., Jayaprakasha, G.K., Patil, B., Qian, X., Koiwa, H., 2021. Transition of aromatic volatile and transcriptome profiles during melon fruit ripening. Plant Sci. 304, 110809 https://doi.org/10.1016/j.plantsci.2020.110809.
Nagashima, Y., Niyakan, S., He, K., Singh, J., Metrani, R., Crosby, K.M., Jifon, J., Jayaprakasha, G., Patil, B., Qian, X., Koiwa, H., 2022. Differential expression of transcription factors in developing melon fruits, melon breeding and genetics: developments in food quality & safety. Am. Chem. Soc. 3–21. https://doi.org/10.1021/bk-2022-1415.ch001.
Ning, M., Tang, F., Chen, J., Song, W., Zhao, X., Zhang, Q., Cai, W., Shan, C., Li, Z., 2022. Physiological and transcriptomic analysis of postharvest Jiashi melon at different storage temperatures. Postharvest Biol. Technol. 191, 111963 https://doi.org/10.1016/j.postharvbio.2022.111963.
Oren, E., Tzuri, G., Dafna, A., Rees, E.R., Song, B., Freilich, S., Elkind, Y., Isaacson, T., Schaffer, A.A., Tadmor, Y., Burger, J., Buckler, E.S., Gur, A., 2022. QTL mapping and genomic analyses of earliness and fruit ripening traits in a melon Recombinant Inbred Lines population supported by de novo assembly of their parental genomes. Hortic. Res. 9 https://doi.org/10.1093/hr/uhab081 uhab081.
Ritchie, M.E., Phipson, B., Wu, D., Hu, Y., Law, C.W., Shi, W., Smyth, G.K., 2015. limma powers differential expression analyses for RNA-sequencing and microarray studies. Nuc. Acids Res. 43 https://doi.org/10.1093/nar/gkv007 e47-e47.
Saladié, M., Cañizares, J., Phillips, M.A., Rodriguez-Concepcion, M., Larrigaudière, C., Gibon, Y., Stitt, M., Lunn, J.E., Garcia-Mas, J., 2015. Comparative transcriptional profiling analysis of developing melon (Cucumis melo L.) fruit from climacteric and non-climacteric varieties. BMC Genom. 16, 440. https://doi.org/10.1186/s12864-015-1649-3.
Schemberger, M.O., Stroka, M.A., Reis, L., de Souza Los, K.K., de Araujo, G.A.T., Sfeir, M. Z.T., Galvão, C.W., Etto, R.M., Baptistão, A.R.G., Ayub, R.A., 2020. Transcriptome profiling of non-climacteric 'yellow' melon during ripening: insights on sugar metabolism. BMC Genom. 21 https://doi.org/10.1186/s12864-020-6667-0, 262-262.
Shin, A.Y., Kim, Y.M., Koo, N., Lee, S.M., Nahm, S., Kwon, S.Y., 2017. Transcriptome analysis of the oriental melon (Cucumis melo L. var. makuwa) during fruit development. PeerJ 5. https://doi.org/10.7717/peerj.2834 e2834-e2834.
Singh, J., Metrani, R., Jayaprakasha, G.K., Crosby, K.M., Ravishankar, S., Patil, B.S., 2020. Multivariate analysis of amino acids and health beneficial properties of cantaloupe varieties grown in six locations in the United States. Plants 9. https://doi.org/10.3390/plants9091058 (Basel).
Singh, J., Jayaprakasha, G.K., Patil, B.S., 2021. Improved sample preparation and optimized solvent extraction for quantitation of carotenoids. Plant Foods Hum. Nutr. 76, 60–67. https://doi.org/10.1007/s11130-020-00862-8.
Singh, J., Metrani, R., Jayaprakasha, G.K., Crosby, K.M., Jifon, J.L., Ravishankar, S., Brierley, P., Leskovar, D.L., Turini, T.A., Schultheis, J., Coolong, T., Guan, W., Patil, B.S., 2022. Profiling carotenoid and sugar contents in unique Cucumis melo L. cultigens harvested from different climatic regions of the United States. J. Food Comp. Anal. 106, 104306 https://doi.org/10.1016/j.jfca.2021.104306.
Tabara, M., Nagashima, Y., He, K., Qian, X., Crosby, K.M., Jifon, J., Jayaprakasha, G.K., Patil, B., Koiwa, H., Takahashi, H., Fukuhara, T., 2021. Frequent asymptomatic infection with tobacco ringspot virus on melon fruit. Virus Res. 293, 198266 https://doi.org/10.1016/j.virusres.2020.198266.
Tibshirani, R., 1988. Estimating transformations for regression via additivity and variance stabilization. J. Am. Stat. Assoc. 83, 394–405. https://doi.org/10.1080/01621459.1988.10478610.

Vallone, S., Sivertsen, H., Anthon, G.E., Barrett, D.M., Mitcham, E.J., Ebeler, S.E., Zakharov, F., 2013. An integrated approach for flavour quality evaluation in muskmelon (Cucumis melo L. reticulatus group) during ripening. Food Chem. 139, 171–183. https://doi.org/10.1016/j.foodchem.2012.12.042.

Wang, M., Zhang, L., Boo, K.H., Park, E., Drakakaki, G., Zakharov, F., 2019. PDC1, a pyruvate/alpha-ketoacid decarboxylase, is involved in acetaldehyde, propanal and pentanal biosynthesis in melon (Cucumis melo L.) fruit. Plant J. 98, 112–125. https://doi.org/10.1111/tpj.14204.

Wold, S., Esbensen, K., Geladi, P., 1987. Principal component analysis. Chemometr. Intell. Lab. Syst. 2, 37–52. https://doi.org/10.1016/0169-7439(87)80084-9.

Wu, Z., Shi, Z., Yang, X., Xie, C., Xu, J., Yu, Z., 2022. Comparative metabolomics profiling reveals the molecular information of whole and fresh-cut melon fruit (cv. Xizhoumi-17) during storage. Sci. Hortic. 296, 110914 https://doi.org/10.1016/j.scienta.2022.110914.

Zhang, H., Wang, H., Yi, H., Zhai, W., Wang, G., Fu, Q., 2016. Transcriptome profiling of Cucumis melo fruit development and ripening. Hortic. Res. 3, 16014. https://doi.org/10.1038/hortres.2016.14.

Zhang, S., Nie, L., Zhao, W., Cui, Q., Wang, J., Duan, Y., Ge, C., 2019. Metabolomic analysis of the occurrence of bitter fruits on grafted oriental melon plants. PLoS One 14. https://doi.org/10.1371/journal.pone.0223707 e0223707-e0223707.

Zhang, A., Zheng, J., Chen, X., Shi, X., Wang, H., Fu, Q., 2021. Comprehensive analysis of transcriptome and metabolome reveals the flavonoid metabolic pathway is associated with fruit peel coloration of melon. Molecules 26, 2830.

Zhao, G., Lian, Q., Zhang, Z., Fu, Q., He, Y., Ma, S., Ruggieri, V., Monforte, A.J., Wang, P., Julca, I., Wang, H., Liu, J., Xu, Y., Wang, R., Ji, J., Xu, Z., Kong, W., Zhong, Y., Shang, J., Pereira, L., Argyris, J., Zhang, J., Mayobre, C., Pujol, M., Oren, E., Ou, D., Wang, J., Sun, D., Zhao, S., Zhu, Y., Li, N., Katzir, N., Gur, A., Dogimont, C., Schaefer, H., Fan, W., Bendahmane, A., Fei, Z., Pitrat, M., Gabaldón, T., Lin, T., Garcia-Mas, J., Xu, Y., Huang, S., 2019. A comprehensive genome variation map of melon identifies multiple domestication events and loci influencing agronomic traits. Nat. Genet. 51, 1607–1615. https://doi.org/10.1038/s41588-019-0522-8.

Zheng, Y., Wu, S., Bai, Y., Sun, H., Jiao, C., Guo, S., Zhao, K., Blanca, J., Zhang, Z., Huang, S., Xu, Y., Weng, Y., Mazourek, M., K Reddy, U., Ando, K., McCreight, J.D., Schaffer, A.A., Burger, J., Tadmor, Y., Katzir, N., Tang, X., Liu, Y., Giovannoni, J.J., Ling, K.S., Wechter, W.P., Levi, A., Garcia-Mas, J., Grumet, R., Fei, Z., 2019. Cucurbit genomics database (CuGenDB): a central portal for comparative and functional genomics of cucurbit crops. Nuc. Acids Res. 47 https://doi.org/10.1093/nar/gky944. D1128-D1136.